

# Real-time scanning Hall probe microscopy

A. Oral and S. J. Bending

*School of Physics, University of Bath, Claverton Down, Bath BA2 7AY, United Kingdom*

M. Henini

*Department of Physics, University of Nottingham, Nottingham NG7 2RD, United Kingdom*

(Received 20 May 1996; accepted for publication 3 July 1996)

We describe a low-noise scanning Hall probe microscope having unprecedented magnetic field sensitivity ( $\sim 2.9 \times 10^{-8}$  T/ $\sqrt{\text{Hz}}$  at 77 K), high spatial resolution, ( $\sim 0.85$   $\mu\text{m}$ ), and operating in real-time ( $\sim 1$  frame/s) for studying flux profiles at surfaces. A submicron Hall probe manufactured in a GaAs/AlGaAs two-dimensional electron gas (2DEG) is scanned over the sample to measure the surface magnetic fields using conventional scanning tunneling microscopy positioning techniques. Flux penetration into a high  $T_c$  YBa<sub>2</sub>Cu<sub>3</sub>O<sub>7- $\delta$</sub>  thin film has been observed in real time at 85 K with single vortex resolution. Flux is seen to enter the film in the form of vortex bundles as well as single flux quanta,  $\Phi_0$ . © 1996 American Institute of Physics. [S0003-6951(96)03835-1]

Various techniques have been developed to investigate the surface magnetic structure of materials, including Hall probes,<sup>1</sup> scanning SQUID,<sup>2</sup> and magnetic force (MFM)<sup>3,4</sup> microscopies, Bitter decoration,<sup>5</sup> Faraday rotation,<sup>6</sup> magneto-optic Kerr effect<sup>7</sup> and electron holography.<sup>8</sup> Recently, the scanning Hall probe microscopy (SHPM)<sup>9-11</sup> has been shown to be a very sensitive, noninvasive instrument with which to obtain quantitative measurements of surface magnetic field profiles with high spatial resolution ( $< 1$   $\mu\text{m}$ ) under variable temperature and magnetic field operation. The earliest implementations<sup>9,10</sup> of this instrument had, however, rather limited sensitivity and bandwidth. In this letter, we describe a fast low noise scanning Hall probe microscope which has at least two orders of magnitude better field sensitivity than previous versions<sup>9,10</sup> and can operate in real time,  $\sim 1$  frame/s. Our microscope has a field resolution of  $\sim 2.9 \times 10^{-8}$  T/ $\sqrt{\text{Hz}}$  and wide measurement bandwidth,  $\sim 10$  kHz at 77 K and has even been successfully operated at room temperature.<sup>11</sup> Here we show that real-time SHPM can be used to image flux penetration into a YBa<sub>2</sub>Cu<sub>3</sub>O<sub>7- $\delta$</sub>  thin film.

The microscope incorporates a Hall probe which is brought into close proximity with the sample surface using scanning tunneling microscopy (STM) positioning techniques. The Hall probe is mounted on the piezotube of a custom manufactured low-temperature STM with a stick-slip coarse approach mechanism and is tilted  $\sim 1^\circ$ – $2^\circ$  with respect to the sample. The active Hall sensor is patterned about 13  $\mu\text{m}$  away from the chip corner which has been coated with a thin layer of gold to serve as a tunneling tip. The sample is first approached until tunneling is established and then the Hall probe is scanned across the surface to measure the magnetic field and the surface topography simultaneously as sketched in Fig. 1 (STM tracking SHPM). Alternatively the sample can be retracted about  $\sim 0.5$   $\mu\text{m}$  and Hall probe scanned much more rapidly to measure the magnetic field profile with a slightly lower spatial resolution (normal SHPM).

The Hall probe is manufactured in a GaAs/Al<sub>0.3</sub>Ga<sub>0.7</sub>As heterostructure two-dimensional electron gas (2DEG) ( $n_{2D} = 2.7 \times 10^{11}$  cm<sup>-2</sup> and  $\mu = 300\,000$  cm<sup>2</sup>/V s at 4.2 K in the

dark). Hall bars with wire widths of 1  $\mu\text{m}$  are microfabricated with optical lithography, yielding an effective electrical width  $\sim 0.85$   $\mu\text{m}$  after sidewall depletion.

A scanning electron micrograph of a Hall probe is shown in Fig. 2. The active Hall sensor is about 13  $\mu\text{m}$  away from the corner of a deep mesa etch, which is coated with gold. The corner of the mesa, not the corner of the chip, serves as a tunnel tip. We have deliberately separated the tip metal coating and Hall bar in contrast to previous SHPM designs<sup>9</sup> where the tip metal was evaporated over the entire Hall probe. This eliminates the gating effect of the tip metal on the Hall probe and dramatically reduces the noise and coupling between tunnel current and Hall signal. We can therefore, simultaneously operate the microscope in STM and SHPM modes. Moreover, the measurement bandwidth is increased dramatically in this configuration.

A PZT-5H piezotube is used for the scanner with a  $\sim 10$   $\mu\text{m}$  scan range at 4.2 K. Bias currents of  $\sim 1$ – $60$   $\mu\text{A}$  are supplied with a precision current source and the Hall voltage is measured with an AD625 low noise instrumentation amplifier. The microscope is placed in a cryostat containing a 1.5–300 K variable temperature insert and a 7 T superconducting magnet. The cryostat is mounted on a double stage vibration isolation system to eliminate external disturbances.

The Hall probes typically have  $\sim 0.3$   $\Omega/\text{G}$  Hall coefficient.

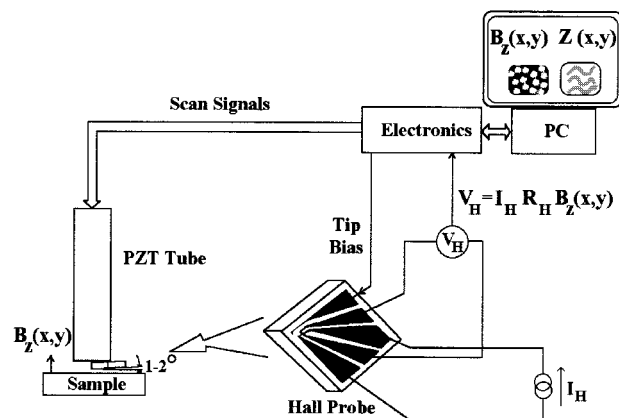


FIG. 1. Schematic diagram of scanning Hall probe microscope.

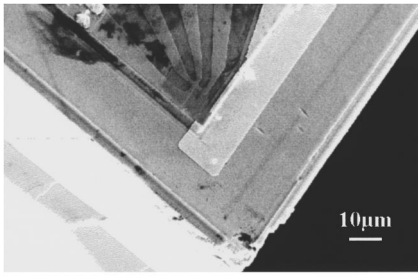


FIG. 2. Scanning electron micrograph of a Hall probe.

cient and the main noise component up to a certain bias current level  $I_{\max}$ , is found to be the Johnson noise,  $V_n = \sqrt{4k_B T R_s f}$ , of the Hall bar where  $R_s$  and  $f$  are the series resistance of Hall probe and measurement bandwidth respectively. Above this current level, the noise is found to increase with current. Therefore, for  $I_{\text{Hall}} < I_{\max}$ , the signal to noise ratio (SNR) of the Hall probe is

$$\text{SNR} = \frac{I_{\text{Hall}} R_H B}{\sqrt{4k_B T R_s f}}, \quad (1)$$

where  $I_{\text{Hall}}, B, R_H$  are the bias current, magnetic field, and Hall coefficient, respectively. Our Hall probes can sustain currents up to  $4 \mu\text{A}$  at 300 K and up to  $60 \mu\text{A}$  below 77 K, without increasing the noise and typical series resistances are 60, 3, and  $1.5 \text{ K}\Omega$  are 300, 77, and 4.2 K, respectively. The magnetic field resolution of the Hall probe is measured to be  $\sim 3.8 \times 10^{-6} \text{ T}/\sqrt{\text{Hz}}$  at 300 K and  $\sim 2.9 \times 10^{-8} \text{ T}/\sqrt{\text{Hz}}$  at 77 K (including the amplifier noise). The flux resolution of the microscope,  $\sim 1 \times 10^{-5} \Phi_0/\sqrt{\text{Hz}}$  at 77 K, is comparable with the best scanning SQUID systems<sup>2</sup> operating at 4.2 K. There is a small  $1/f$  noise component with  $f_c \sim 10 \text{ Hz}$ . The field resolution is expected to be  $\sim 3.1 \times 10^{-9} \text{ T}/\sqrt{\text{Hz}}$  at 4.2 K, but the voltage noise of our amplifier which is  $4 \text{ nV}/\sqrt{\text{Hz}}$  ( $\equiv 2.2 \times 10^{-8} \text{ T}/\sqrt{\text{Hz}}$ ) becomes the dominant noise source below 77 K at the moment. The frequency response of the Hall probe is flat up to  $\sim 10 \text{ kHz}$  at 77 K and then rolls off with 10 dB/decade. The bandwidth is reduced to 1 kHz if high magnetic field resolution is required. Images usually take a couple of minutes to scan in the normal SHPM mode depending on the image size and scanning speed.

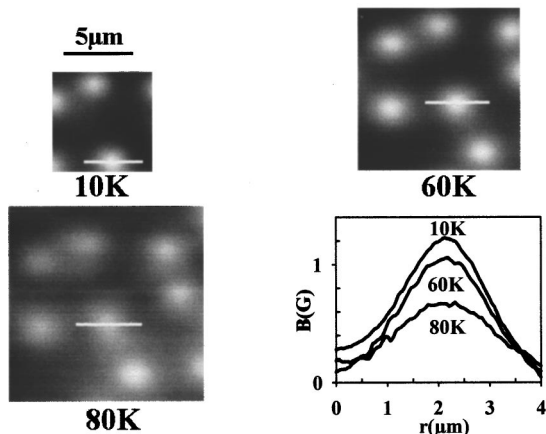
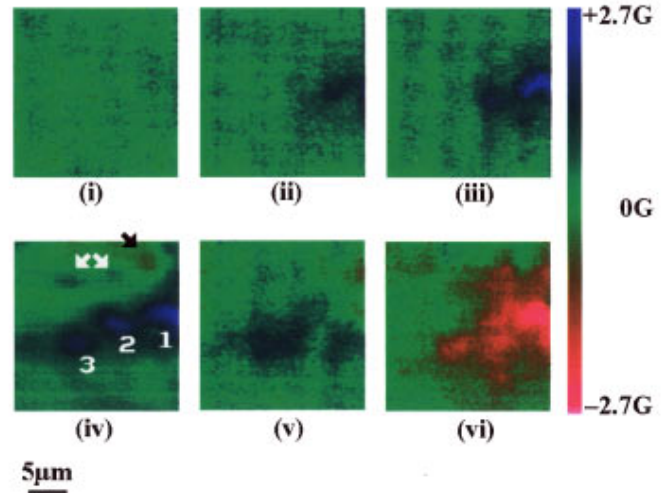
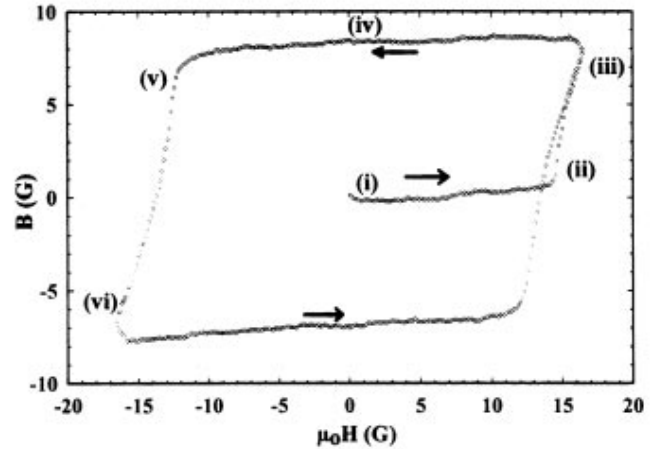


FIG. 3. SHPM images of vortices in a  $\text{YBa}_2\text{Cu}_3\text{O}_{7-\delta}$  thin film at different temperatures and the cross sections of the same vortex along the lines.



(a)



(b)

FIG. 4. (a) Samples of SHPM images of flux penetration into a  $\text{YBa}_2\text{Cu}_3\text{O}_{7-\delta}$  film with the Hall probe positioned  $0.67 \mu\text{m}$  above the film at 85 K, blue represents the positive, green zero, and red negative fields as shown with the color bar (b) a typical hysteresis curve obtained with the Hall probe  $\sim 4.2 \mu\text{m}$  above the surface.

The high quality  $\text{YBa}_2\text{Cu}_3\text{O}_{7-\delta}$  thin film used in this study was grown by electron beam evaporation of the metals in the presence of atomic oxygen on a MgO substrate at  $690^\circ\text{C}$ <sup>12</sup> and had a thickness of  $0.35 \mu\text{m}$  and  $J_c = 1.4 \times 10^6 \text{ A/cm}^2$  at 77 K. The critical temperature of the film was found to be  $\sim 90.4 \text{ K}$  by magnetization measurements performed with the Hall probe itself which agrees well with the  $90.8 \text{ K}$  measured by dc magnetization measurements on the whole sample. These properties suggest that the sample

was close to optimal doping or perhaps slightly underdoped. Figure 3 shows SHPM images of vortices trapped in the  $\text{YBa}_2\text{Cu}_3\text{O}_{7-\delta}$  thin film at various temperatures with the Hall probe positioned  $0.67 \mu\text{m}$  above the film. The scanning range drops at low temperatures due to a reduction in the piezoelectric coefficient of the tube and was calibrated prior to the experiments by scanning a grating in STM mode. The sample was field cooled at  $+1 \text{ G}$ . As the temperature is reduced, the penetration depth is seen to decrease and the vortices start to sharpen up. The cross sections along the same vortex at different temperatures are also displayed in the figure to demonstrate the performance. The London penetration depth  $\lambda$ , of the superconductor, its temperature dependence and its *local* variations across the surface can all be measured microscopically from these profiles.<sup>13</sup>

The noise figures and the wide frequency response of the Hall probe allows the possibility of real-time operation with reasonably high scan rates of  $\sim 1$  frame/s, even at  $T=85 \text{ K}$ . The measurement bandwidth is increased to  $10 \text{ kHz}$  during real-time operation and the same area is scanned successively and images are directly dumped into the hard disk of the PC. We have observed the penetration of flux into  $\text{YBa}_2\text{Cu}_3\text{O}_{7-\delta}$  thin films with SHPM in real time with single vortex resolution. The sample is first zero field cooled to  $85 \text{ K}$ . The external field is then cycled to  $+16.5 \text{ G}$ , then decreased to  $-16.5 \text{ G}$  and finally brought back to  $+16.5 \text{ G}$ , while imaging the sample continuously. The sample size is  $5 \times 5 \text{ mm}$  and the Hall probe is positioned  $\sim 2 \text{ mm}$  from the edge of sample. The image size and scan area are  $128 \times 128$  pixels and  $\sim 25 \times 25 \mu\text{m}$ , respectively. Each image took  $1.4 \text{ s}$  to acquire and there were  $\sim 200$  frames during the field sweep. Figure 4(a) shows samples of these images (i)–(vi) corresponding to different positions on the magnetization curve given in Fig. 4(b). The magnetization measurement displayed in Fig. 4(b) is made with the same Hall probe positioned  $\sim 4.2 \mu\text{m}$  away from the surface and represents a typical local  $B$ – $H$  curve for a type-II superconductor. The striations on some of the images are artefacts arising from the electronics because of the very high scan speed. Image (i) in Fig. 4(a) shows the virgin state of superconductor after zero field cooling with no flux evident. As the external field increases the flux is clearly seen to enter from the right in the form of localized bundles [labeled in image (iv) of Fig. 4(a)]. Bundle 1 in image (ii) first grows to a few microns in diameter and then a large number of vortices suddenly jump to position 2 [image (iii)]. Bundle 2 then grows in turn and there is a second jump to position 3 sometime later [image (iv)]. Two isolated vortices (white arrows) and an antivortex (black arrow) can also be clearly resolved in this image. This antivortex was possibly created during the zero field cooling

and might have been attracted into the scan area by vortex–antivortex interactions. Alternatively it might have been generated at the edge of the sample as the field was reduced from  $+16.5 \text{ G}$  down to zero as predicted by recent theories of the field distribution in a thin type II superconducting strip.<sup>14</sup> The bundles are typically  $4$ – $5 \mu\text{m}$  in diameter and contain between 3 and 10 vortices. Upon field reversal, bundles of antivortices are seen to enter along the same route, leading eventually to vortex–antivortex annihilation and the formation of antivortex bundles [images (v) and (vi)].

In conclusion, we have constructed a scanning Hall probe microscope with unprecedented figures of merit. Flux penetration into a  $\text{YBa}_2\text{Cu}_3\text{O}_{7-\delta}$  thin film has been successfully imaged in real time with single vortex resolution. The flux is seen to penetrate mainly in the form of bundles containing 3–10 vortices at  $85 \text{ K}$ . However, the penetration of single flux quanta,  $\Phi_0$ , is not uncommon.

We acknowledge fruitful discussions with H. F. Hess and A. A. Chang. We would like to thank R. G. Humphreys and N. G. Chew of DRA Malvern for supplying the  $\text{YBa}_2\text{Cu}_3\text{O}_{7-\delta}$  film.

This work was supported in the United Kingdom by EPSRC and MOD Grant No. GR/J03077 and the University of Bath through the initiative fund.

- <sup>1</sup>H. T. Coffey, *Cryogenics* **7**, 73 (1965); R. N. Goren and M. Tinkham, *J. Low Temp. Phys.* **5**, 465 (1971).
- <sup>2</sup>C. C. Tsuei, J. R. Kirtley, C. C. Chi, L. S. Yu-Jahnes, A. Gupta, T. Shaw, J. Z. Sun, and M. B. Ketchen, *Phys. Rev. Lett.* **73**, 593 (1994).
- <sup>3</sup>Y. Martin, D. Rugar, and H. K. Wickramasinghe, *Appl. Phys. Lett.* **52**, 244 (1988).
- <sup>4</sup>A. Moser, H. J. Hug, I. Parashikov, B. Stiefel, O. Fritz, H. Thomas, A. Varatoff, H.-J. Guntherodt, and P. Chaudhari, *Phys. Rev. Lett.* **74**, 1847 (1995).
- <sup>5</sup>G. J. Dolan, F. Holtzberg, C. Field, and T. R. Dinger, *Phys. Rev. Lett.* **62**, 2184 (1989).
- <sup>6</sup>P. B. Alers, *Phys. Rev.* **105**, 104 (1957).
- <sup>7</sup>A. A. Polyanskii, A. Gurevic, A. E. Pashitski, N. F. Heinig, R. D. Redwing, J. E. Nordman, and D. C. Larbalestier, *Phys. Rev. B* **53**, 8687 (1996).
- <sup>8</sup>T. Matsuda, A. Fukuhara, T. Yoshioka, S. Hasegawa, A. Tonomura, and Q. Ru, *Phys. Rev. Lett.* **66**, 457 (1991).
- <sup>9</sup>A. M. Chang, H. D. Hallen, L. Harriot, H. F. Hess, H. L. Loa, J. Kao, R. E. Miller, and T. Y. Chang, *Appl. Phys. Lett.* **61**, 1974 (1992).
- <sup>10</sup>D. Davidovic, S. Kumar, K. H. Reich, J. Siegel, S. B. Field, R. D. Tiberio, R. Hey, and K. Ploog, *Phys. Rev. Lett.* **76**, 815 (1996).
- <sup>11</sup>A. Oral, S. J. Bending, and M. Henini, *J. Vac. Sci. Technol. B* **14**, 1202 (1996).
- <sup>12</sup>N. G. Chew, J. A. Edwards, R. G. Humphreys, J. S. Satchell, S. W. Goodyear, B. Dew, N. J. Exon, S. Hensen, M. Lenkens, G. Mullen, and S. Orbach-Werbig, *IEEE Trans. Appl. Supercond.* **5**, 1167 (1995).
- <sup>13</sup>A. Oral, S. J. Bending, R. G. Humphreys, and M. Henini (unpublished).
- <sup>14</sup>E. H. Brandt, M. V. Indenbohm, and A. Forkl, *Europhys. Lett.* **22**, 735 (1993).